



山东大学药学院
SCHOOL OF PHARMACEUTICAL SCIENCES
SHANDONG UNIVERSITY

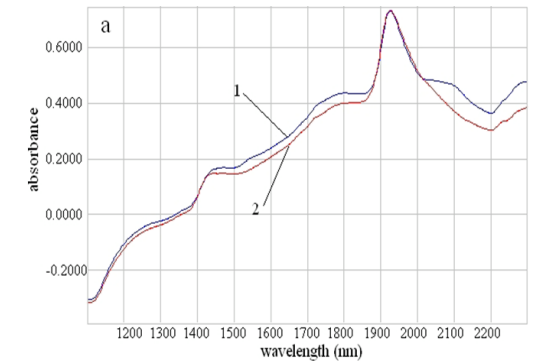
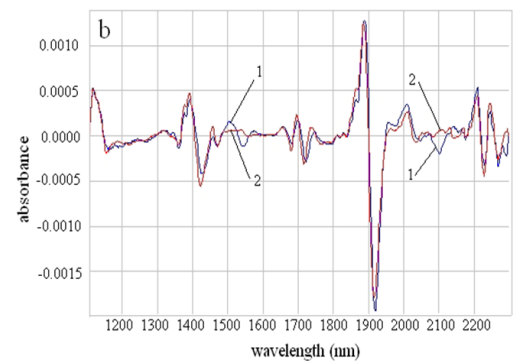
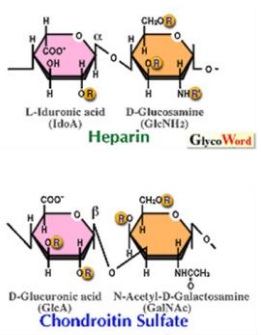
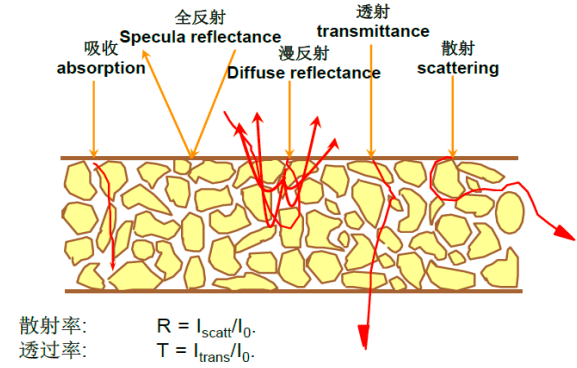
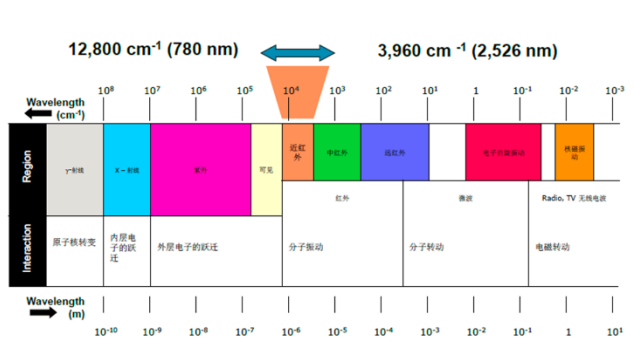
基于水光谱组学的近红外光谱应用研究

汇报人：李连 副研究员
山东大学药学院
lilian@sdu.edu.cn

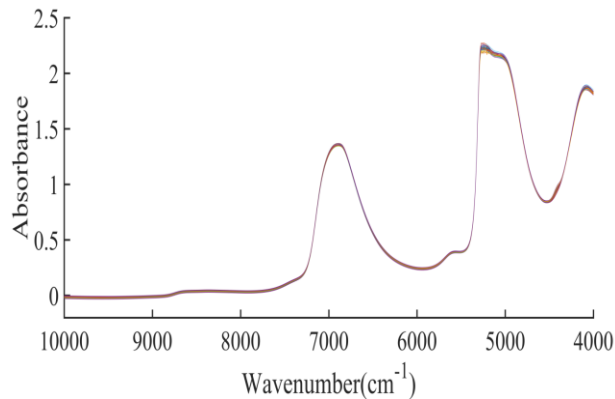
CONTENTS

- 1 基础知识简介
- 2 应用简介
- 3 展望

近红外光谱



近红外光谱



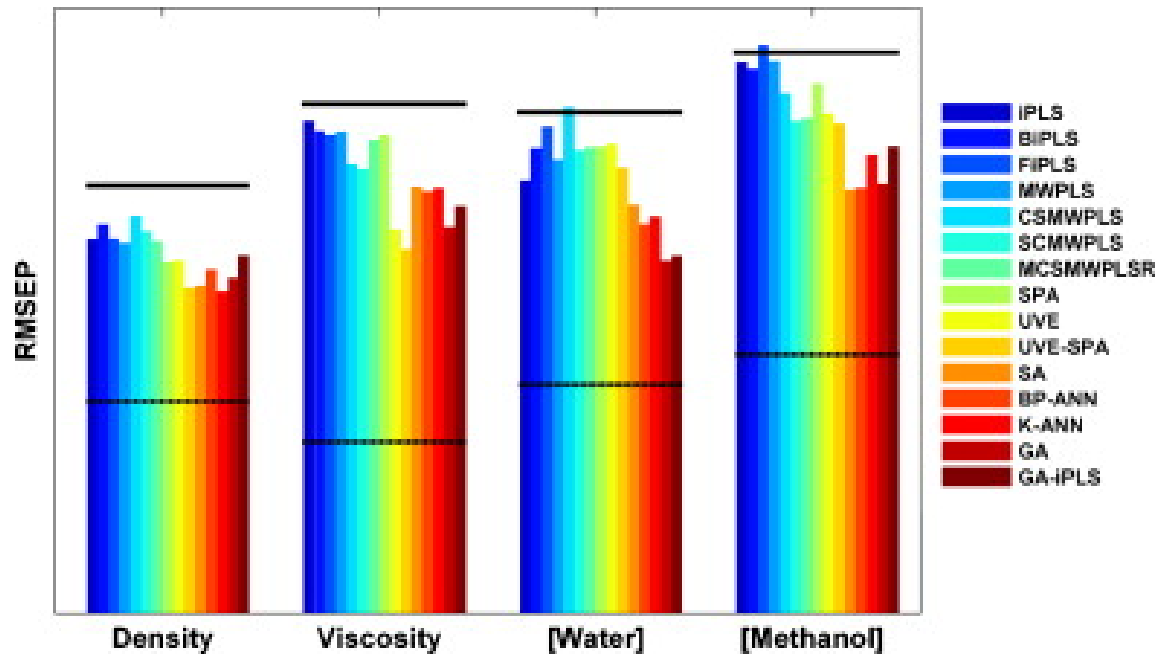
如何寻找有用的信息？

两个主要的方式：

消除背景的影响，直接挖掘有效信息

利用背景的知识，间接反映有效信息

变量选择

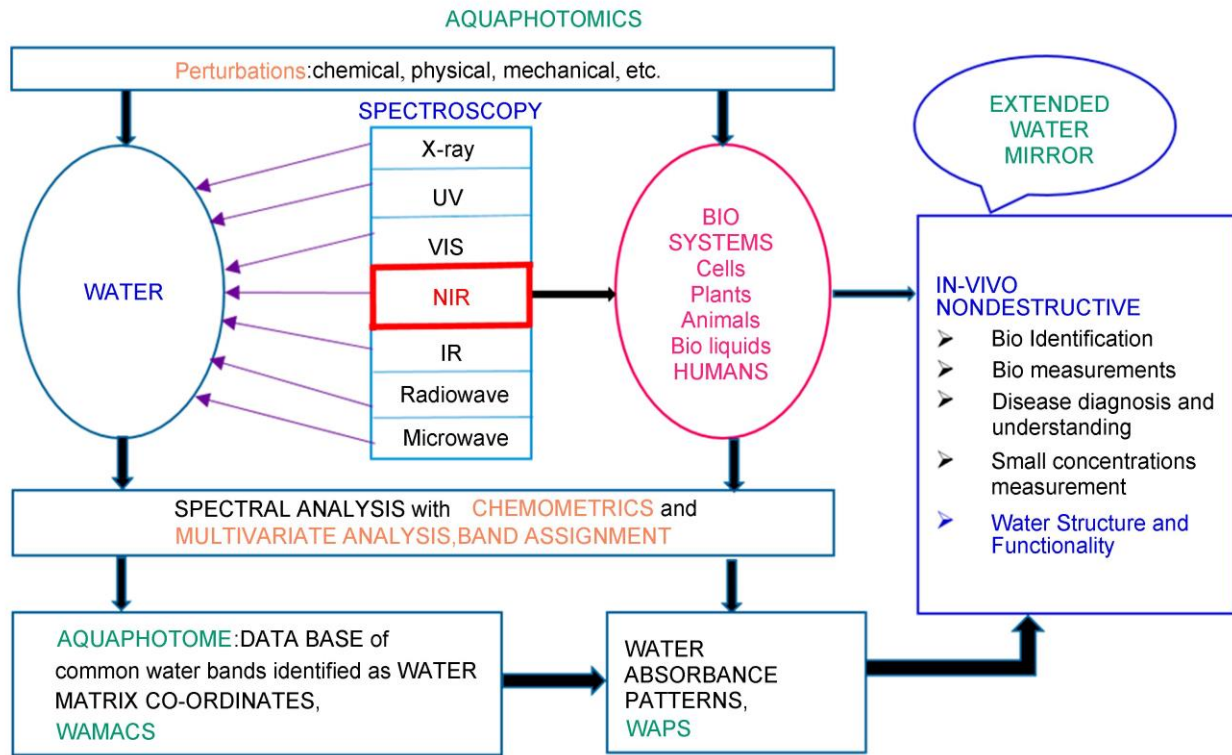


The comparison of fifteen (15) feature selection methods based on partial least squares (PLS) regression for biodiesel analysis. The results are presented for density, viscosity, water content, and methanol content. Thick horizontal lines represent full-spectrum PLS data, and dotted horizontal lines represent full-spectrum artificial neural network (ANN) results. The RMSEP for density and viscosity prediction is multiplied by 100 and 500, respectively, to permit plotting these results with water and methanol errors.

水光谱组学

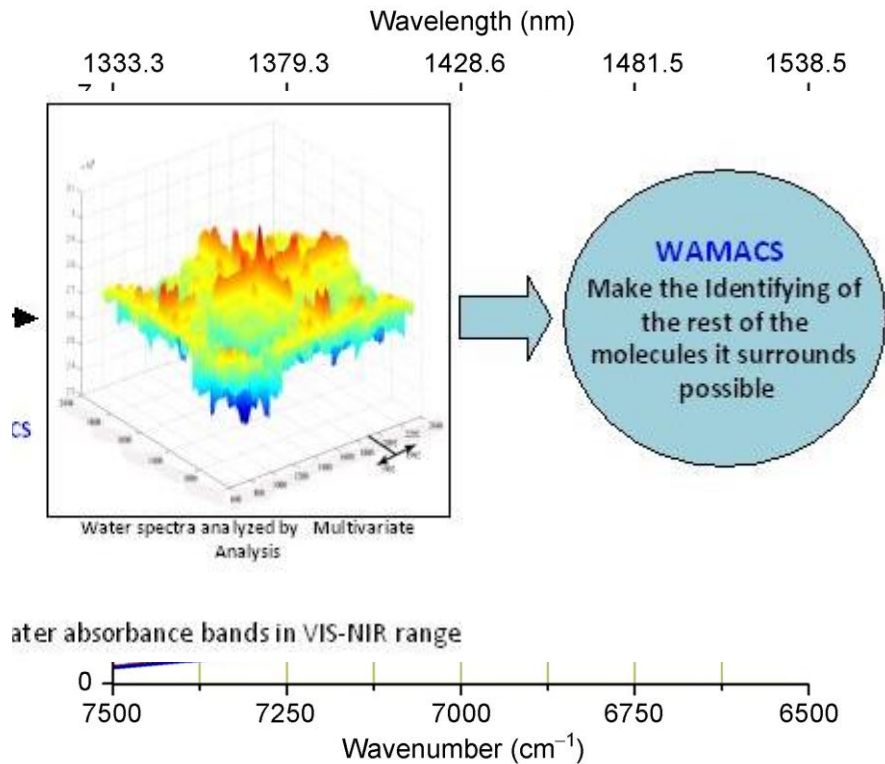


Aqua - : water Prof. Tsenkova
Photo - : light
Omics - : all about,
complement of something



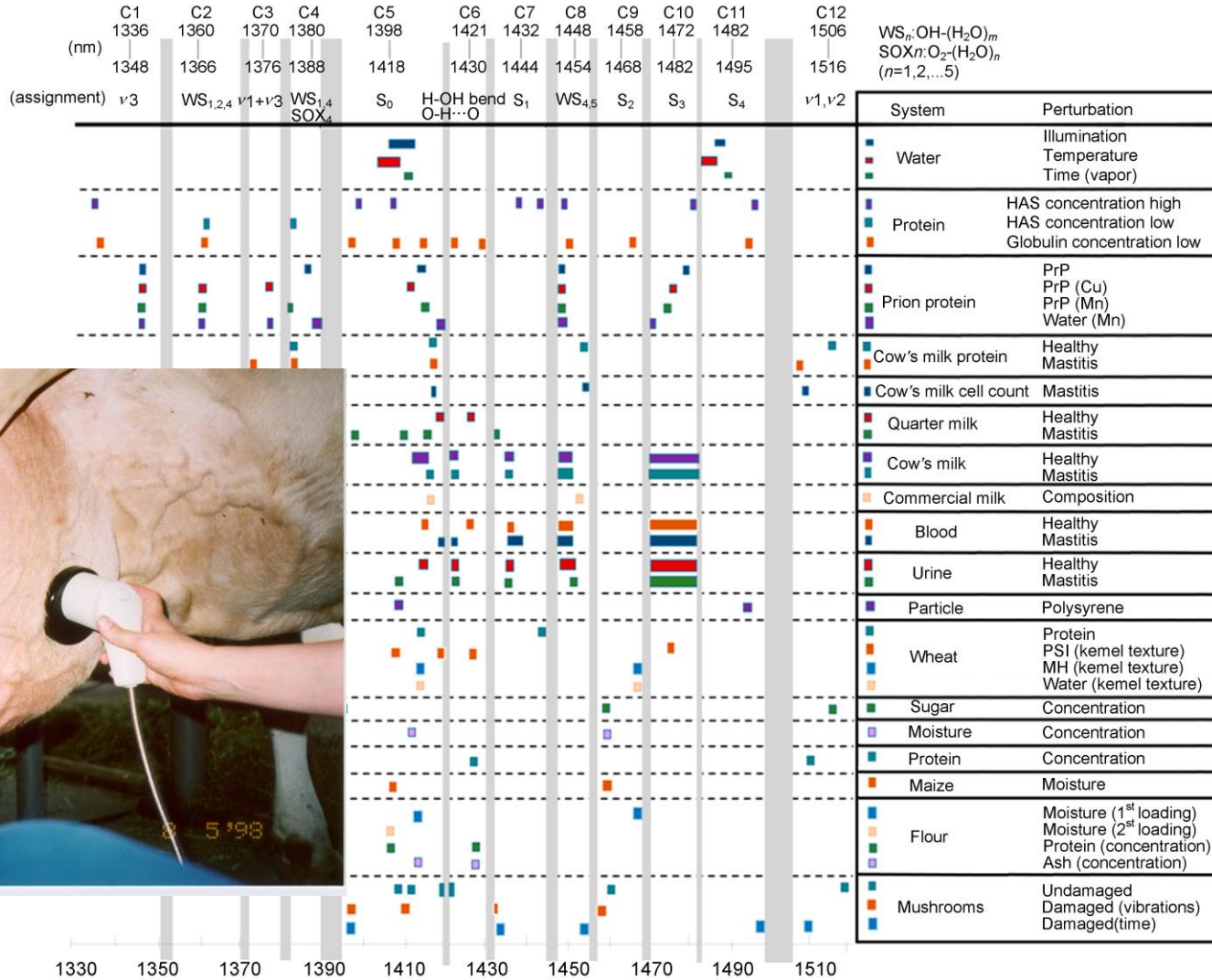
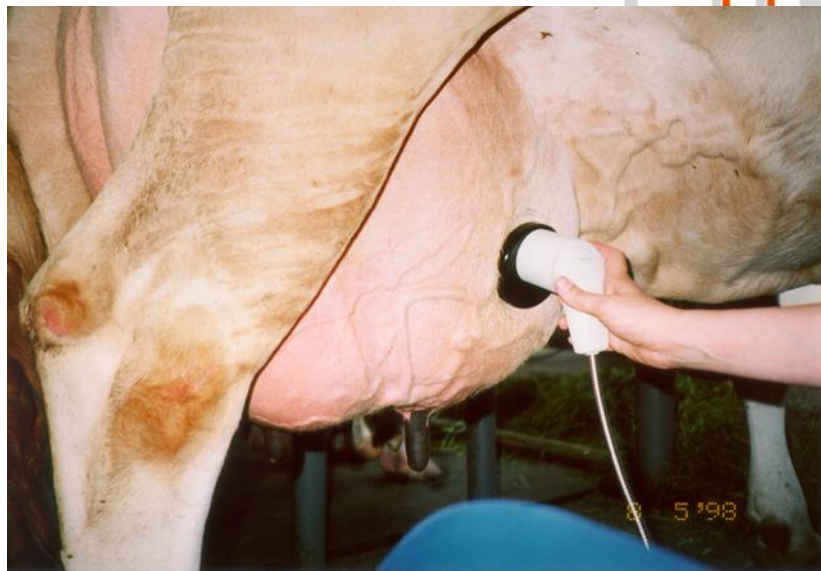
WAMACS

- 1336-1348 nm ($\nu_3(\text{OH})$ 的反对称伸缩振动)
- 1360-1366 nm ($\text{OH}-(\text{H}_2\text{O})_{1,2,4}$ (OH水化层))
- 1370-1376 nm ($\nu_1+\nu_3$ (对称伸缩+反对称伸缩))
- 1380-1388 nm ($\text{OH}-(\text{H}_2\text{O})_{1,4}$); $\text{O}_2-(\text{H}_2\text{O})_4$)
- 1398-1418 nm (S_0),
- 1421-1430 nm (H-OH bend, O-H...O),
- 1432-1444 nm (S_1)
- 1448-1454 nm ($\text{OH}-(\text{H}_2\text{O})_{4,5}$)
- 1458-1468 nm (S_2)
- 1472-1482 nm (S_3)
- 1495 nm (S_4)

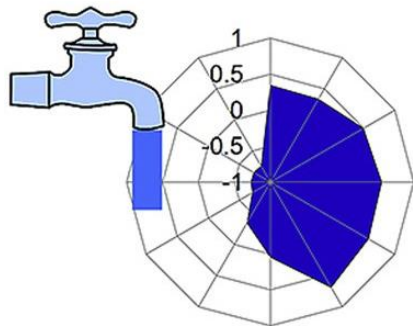
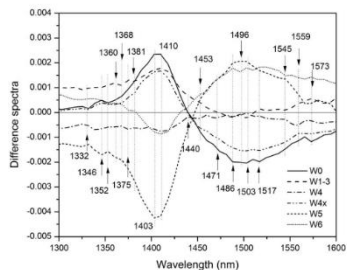


基础知识简介

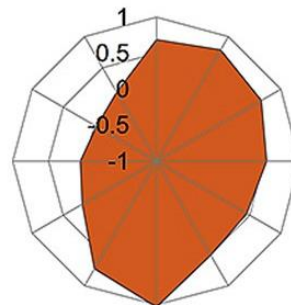
WAMACS



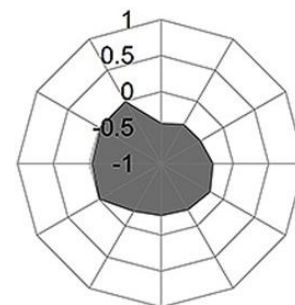
AQUGRAM



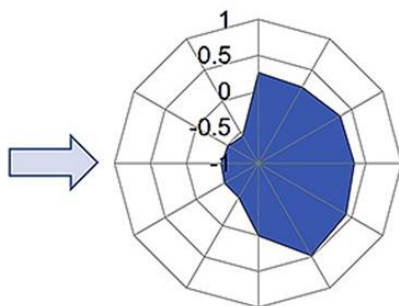
■ Tap water



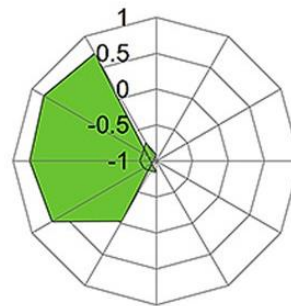
■ Mechanical filtration phase



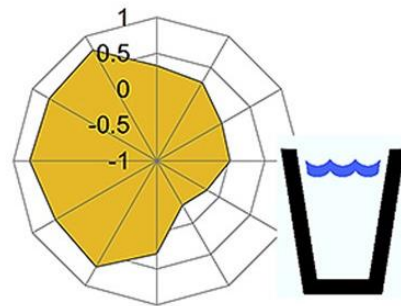
■ Reverse osmosis phase



■ Waste water



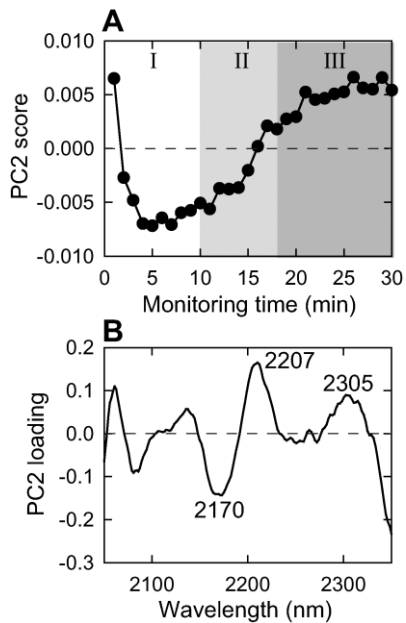
■ Storage phase



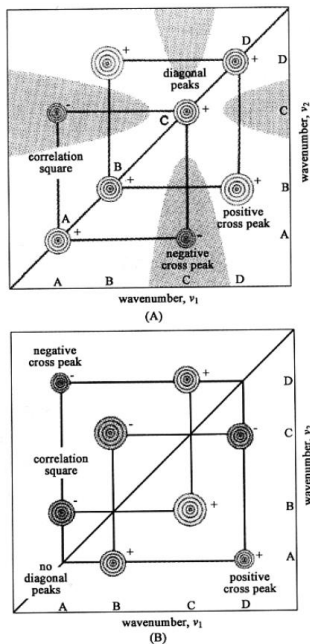
■ Polishing phase - Final product

主要方法

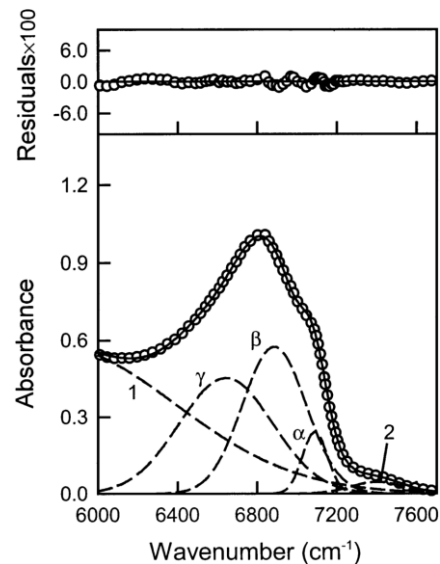
PCA



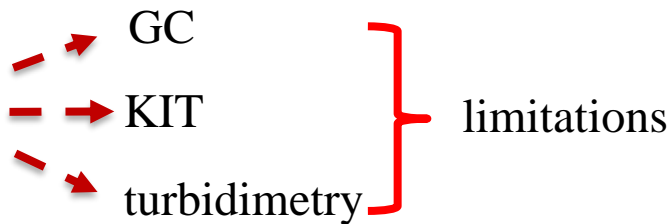
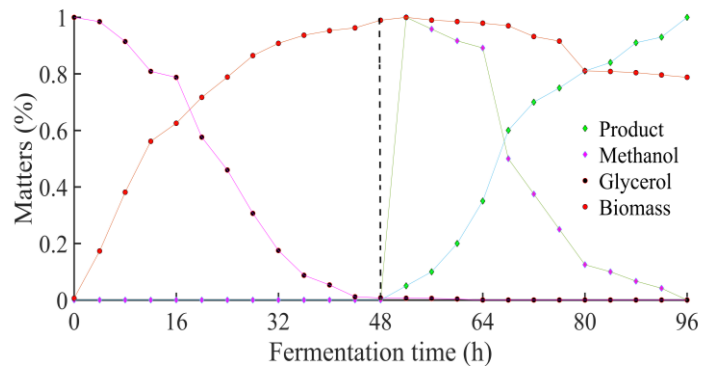
2-D



其它:拟合, 超额光谱, PLS

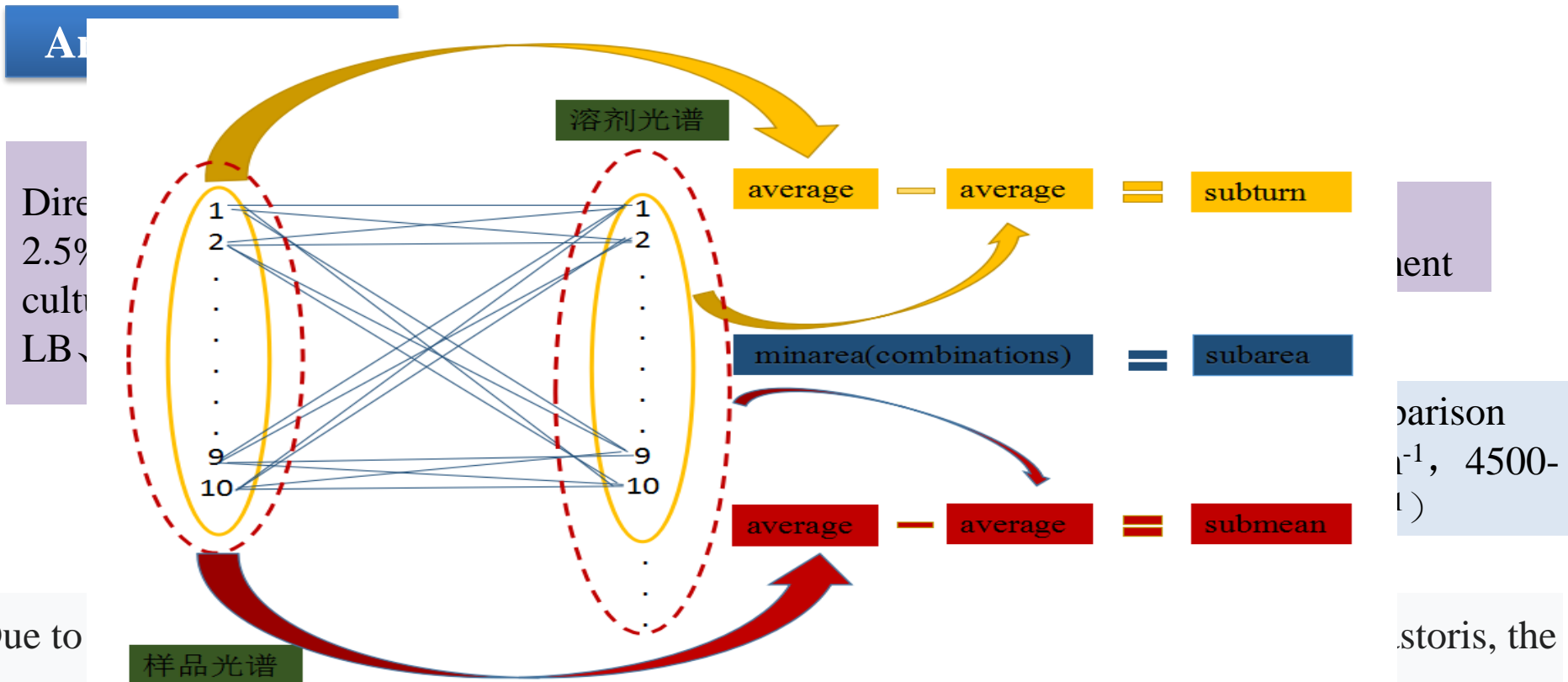


应用简介-发酵过程中多参数的在线检测研究



**NIRS &
Aquaphotomics**

应用简介-发酵过程中多参数的在线检测研究



At

Directly
2.5%
cult
LB

ment

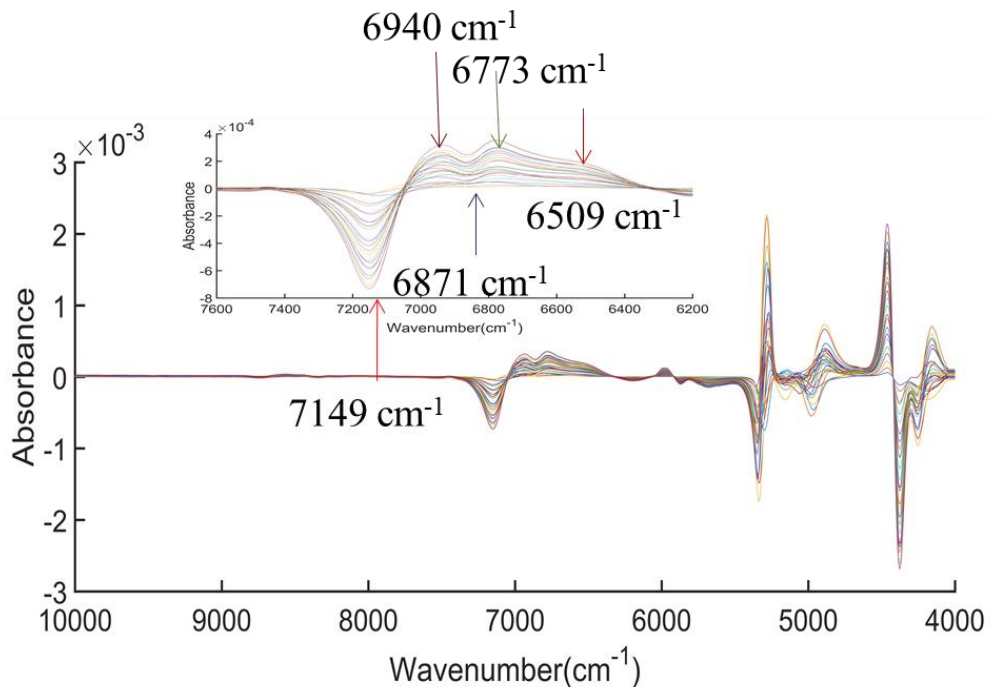
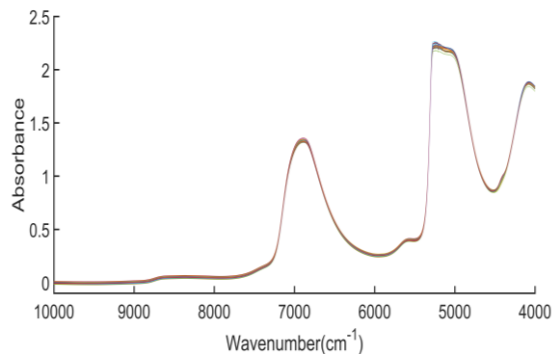
Comparison
($^{-1}$, 4500-
1)

Due to

storis, the

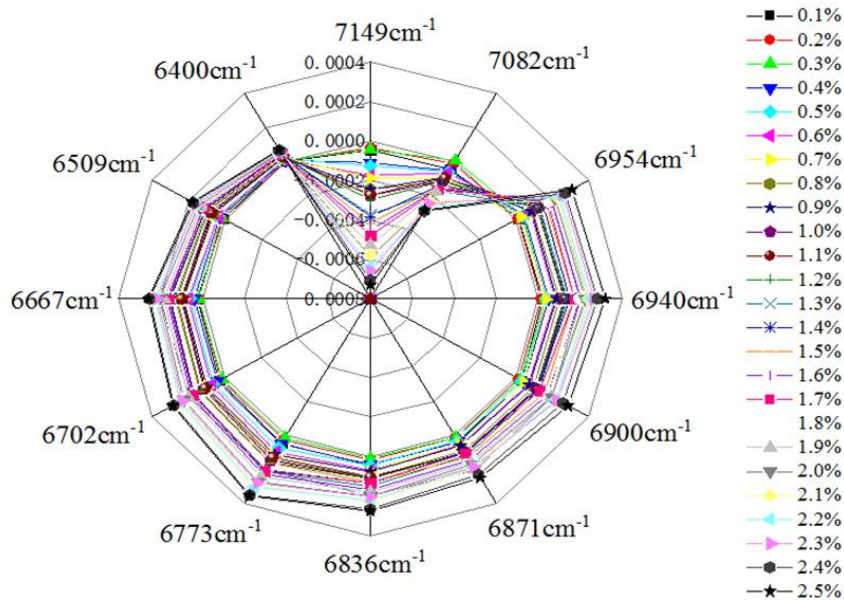
concept of aquaphotomics was introduced and the feasibility of aquaphotomics was investigated.

发酵过程中多参数的在线检测研究



NIR spectra methanol-YPD with a concentration range from 0.1% to 2.5% (v/v) after pre-processing.

应用简介-发酵过程中多参数的在线检测研究



Aquagrams on the spectra between 7600 and 6250 cm^{-1} of methanol-aqueous solutions.

The attribution of the characteristic peaks of water in NIR region

	Wavenumber (cm^{-1})	Attribution
1	7149	The band located between 7168 and 7128 cm^{-1} was called "dehydration band".
2	7082, 6702, 6954	The wavenumbers 7082 cm^{-1} and 6702 cm^{-1} represented two major water species with weaker and stronger hydrogen bonds, respectively. A third species whose concentration was relatively constant as a function of temperature was located at 6954 cm^{-1} .
3	7070	There were no hydrogen bonds in the water molecules-(H_2O) 0.
4	6940	Water clusters contained one hydrogen bonds-(H_2O)1.
5	6900	A broad peak centered near 6900 cm^{-1} consisted of many overlapping bands due to the combinations of OH antisymmetric and symmetric stretching modes.
6	6836, 6711	Water clusters contained two or three hydrogen bonds-(H_2O)2-3.
7	6667	Absorption bands below 6667 cm^{-1} represented highly organized water structures with strong H-bonds.

应用简介-发酵过程中多参数的在线检测研究



Correlation coefficients between the absorbance values of the specific wavenumber and the actual concentration of methanol

wavenumber (cm ⁻¹)	correlation coefficient	wavenumber (cm ⁻¹)	correlation coefficient
7149	0.997	6836	0.972
7082	0.967	6773	0.978
6954	0.985	6702	0.985
6940	0.986	6667	0.988
6900	0.979	6509	0.995
6871	0.969	6400	0.976

12个水基质坐标与浓度呈现良好的线性

performance of model with different preprocessing method

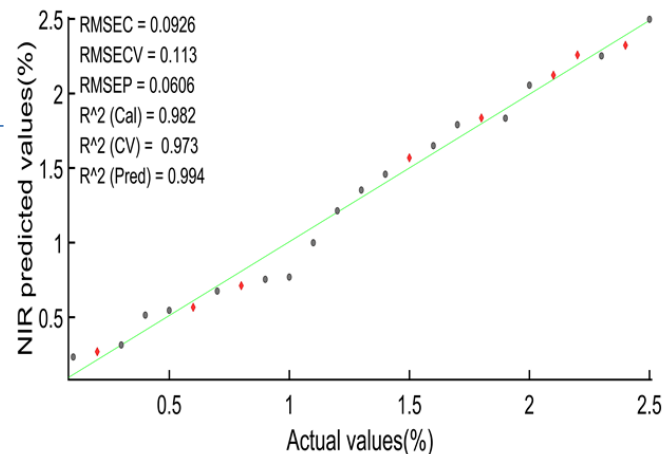
Preprocessing methods	Model performance						
	RMSEC	RMSECV	RMSEP	R _c ²	R _{cv} ²	R _p ²	RPD
autoscaling	0.045	0.052	0.118	0.996	0.995	0.988	6.093
mean center	0.041	0.050	0.123	0.997	0.995	0.988	5.846
SNV ^a	0.529	0.657	0.424	0.481	0.339	0.651	1.696
MSC ^a	0.530	0.688	0.426	0.479	0.337	0.653	1.688
SG(13,1,1) ^{a, b}	0.017	0.044	0.035	0.999	0.996	0.999	20.543
<u>SG(25,2,2)^{a, b}</u>	<u>0.014</u>	<u>0.038</u>	<u>0.047</u>	<u>1.000</u>	<u>0.997</u>	<u>0.999</u>	<u>15.298</u>

预处理方法下的预测结果选择

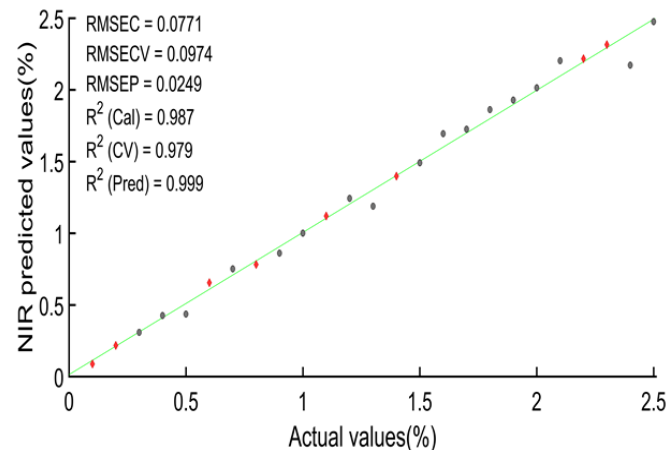
应用简介-发酵过程中多参数的在线检测研究

Model performance in the range of 7600-6250 cm^{-1}

No.	Reference value (%)	Prediction value(%)	Deviation (%)	Relative deviation(%)
1	0.100	0.156	0.056	56.000
2	0.800	0.865	0.065	8.125
3	1.300	1.341	0.041	3.153
4	1.500	1.523	0.023	1.533
5	1.600	1.652	0.052	3.250
6	1.800	1.868	0.068	3.778
7	2.000	2.018	0.018	0.900
8	2.400	2.414	0.014	0.583

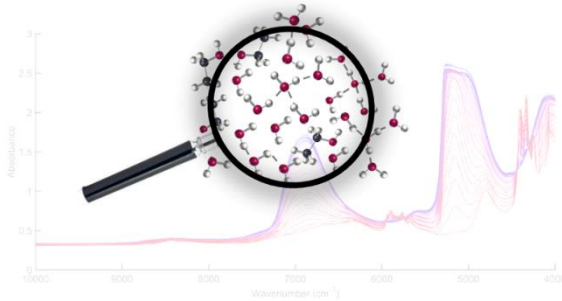


Optimal quantitative model for methanol-LB



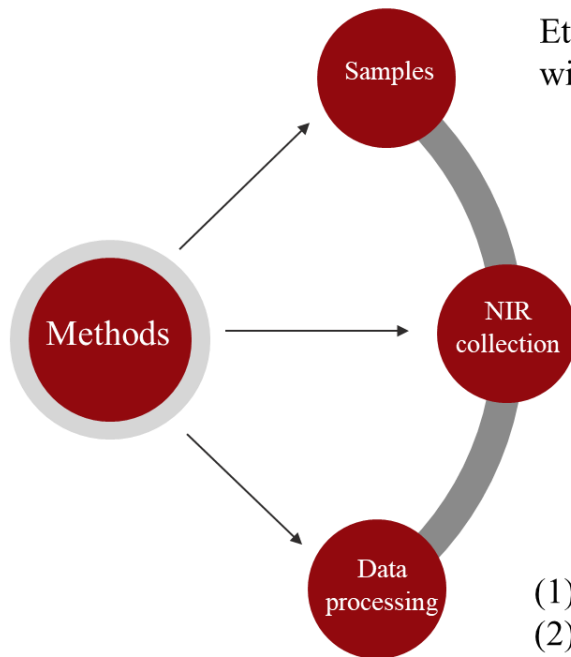
Optimal quantitative model for methanol-YEPG

Alcohol and water undergo incomplete or non-ideal mixing, as shown by the anomalous thermodynamics or physicochemical properties changing nonlinearly with alcohol-water mixing ratio.



A deep understanding of the microscopic behavior of aqueous alcohol solution is indispensable for many chemical and biological processes

应用简介-近红外结合水光谱用于水醇体系的研究



Ethanol-water mixtures of 0-10% with the increment of 1% and 10-100% with 5% increment were prepared using deionized water.

10000 to 4000 cm^{-1} , 1 mm cuvette, 4 cm^{-1} resolution; both an air reference and its spectra were measured, with a scan number of 64. The spectrum of each sample was collected triples and averaged as final spectrum

- (1) Excess spectrum;
- (2) Gaussian fitting based on aquaphtomics;
- (3) 2D-COS;

$$\varepsilon^E = \frac{A}{d(c_1+c_2)} - (x_1\varepsilon_1^* + x_2\varepsilon_2^*)$$

应用简介-近红外结合水光谱用于水醇体系的研究

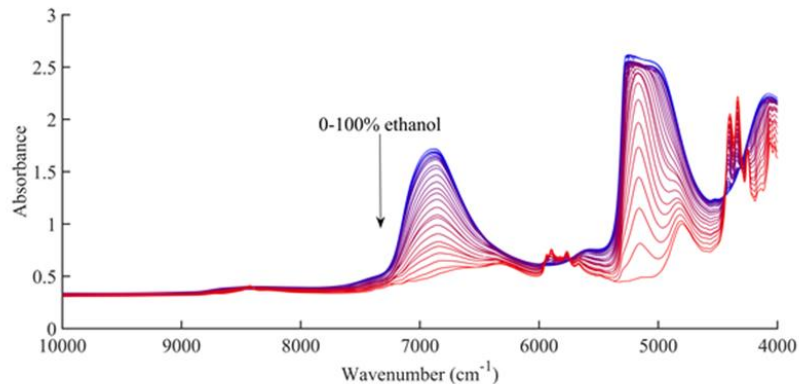
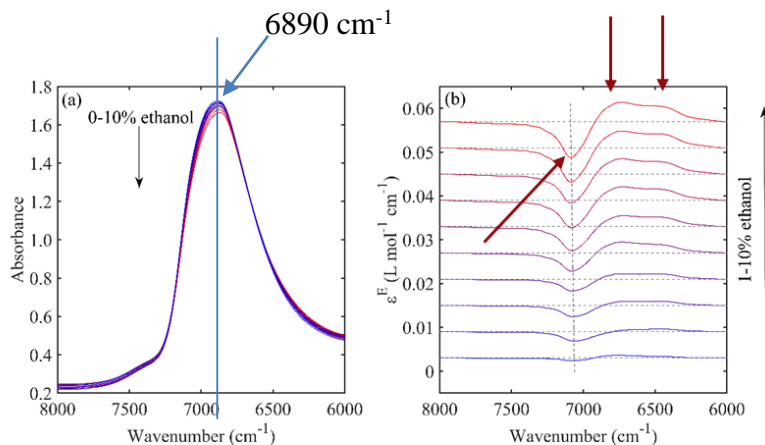


Fig. 1. NIR spectra of ethanol-water mixtures measured over the ethanol concentration of 0-100% (from top to bottom, the spectrum changed from blue to red indicating an increase in ethanol concentration.)⁴

7300-6200 cm^{-1} : the combinations of O-H antisymmetric and symmetric stretching modes of various water species and the first overtones of O-H stretching modes of free and hydrogen bonded ethanol.

Analysis of ethanol-water mixtures in the range of 0-10% ethanol concentration



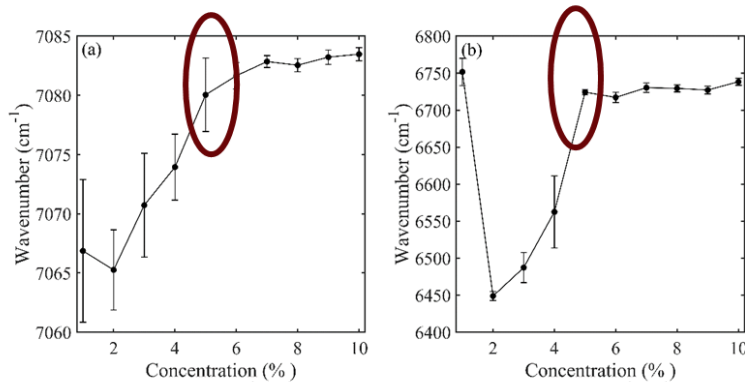
7080 cm⁻¹ : free O-H in water molecules.

6730 cm⁻¹ : first overtone of hydrogen bonded O-H of ethanol;

6420 cm⁻¹: maybe from the O-H of ethanol-water associates

Fig. 2 NIR (a) and excess NIR (b) spectra of the ethanol-water mixtures in the range of the first overtone of O-H groups.

Analysis of ethanol-water mixtures in the range of 0-10% ethanol concentration



dramatic changes when adding ethanol to 5% and 4% respectively;

while ethanol concentration continues to increase, the positions of the positive and negative peaks remain almost

Figure 3. Variation of position for the excess peaks at around 7080 cm⁻¹ (a) and 6730 cm⁻¹ (b) in Fig. 2(b) with ethanol concentration

Gaussian fitting with GA optimization based on aquaphotomics

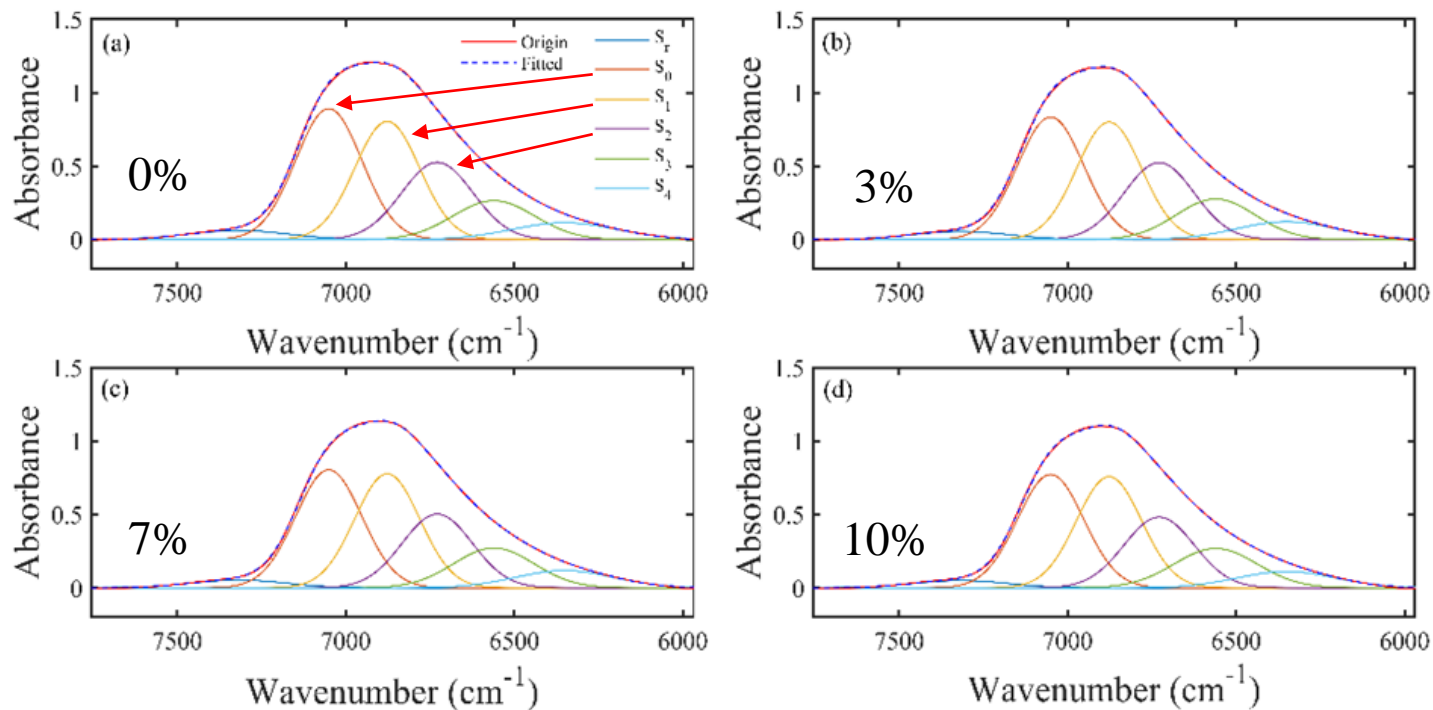
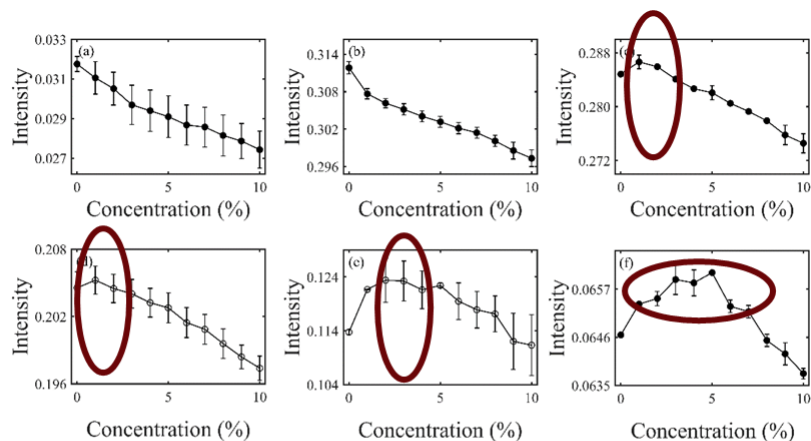


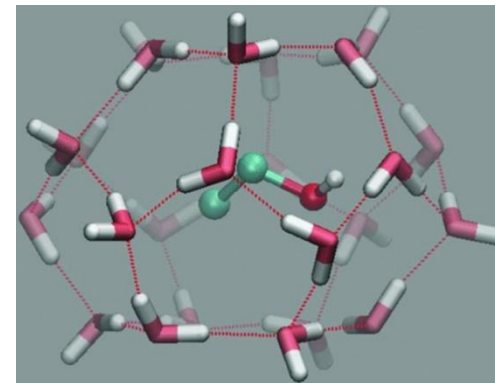
Fig. 5. Variation of the relative intensities for the spectral components including S_r (a), S_0 (b), S_1 (c), S_2 (d), S_3 (e), and S_4 (f) in ethanol-water mixtures with different concentrations of ethanol.



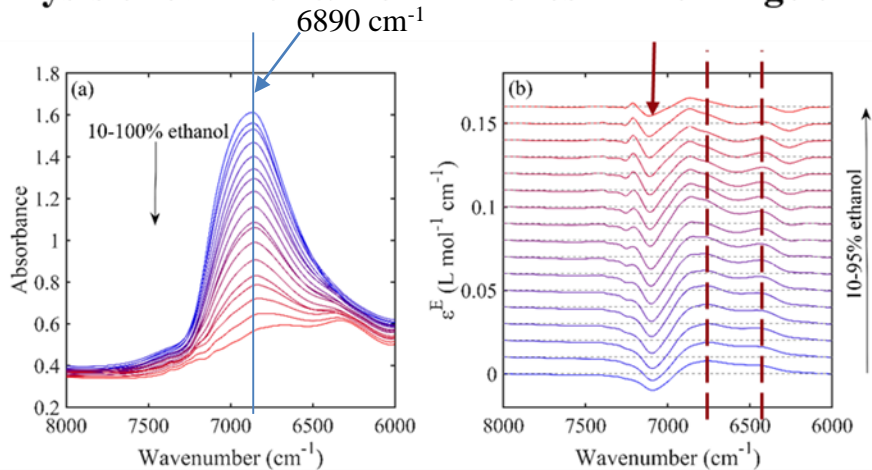
when a small amount of ethanol ($\leq 5\%$) is added into water, hydrophobic hydration plays a major role.

S_1 , S_2 and S_3 : located outside the ethanol hydration shell

Figure 5. Variation of the intensities for the spectral components including S_r (a), S_0 (b), S_1 (c), S_2 (d), S_3 (e), and S_4 (f) in the mixtures with different concentrations of ethanol.



Analysis of ethanol-water mixtures in the range of 10-100% ethanol concentration



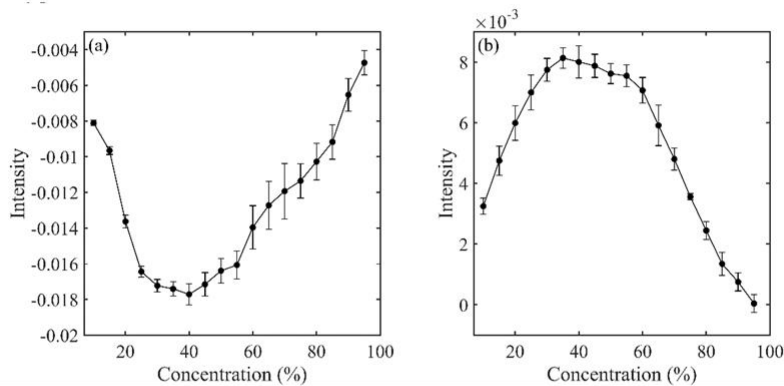
6867 cm⁻¹ ← 6730 cm⁻¹

7080 cm⁻¹: fixed position

6420 cm⁻¹ : O-H absorption of ethanol-water associates.

Figure 6. NIR (a) and excess NIR (b) spectra of ethanol-water mixture. From the blue to red, the volume fraction of ethanol increases from 10 to 100 % with an increment of 5% in (a) and (b).

Analysis of ethanol-water mixtures in the range of 10-100% ethanol concentration



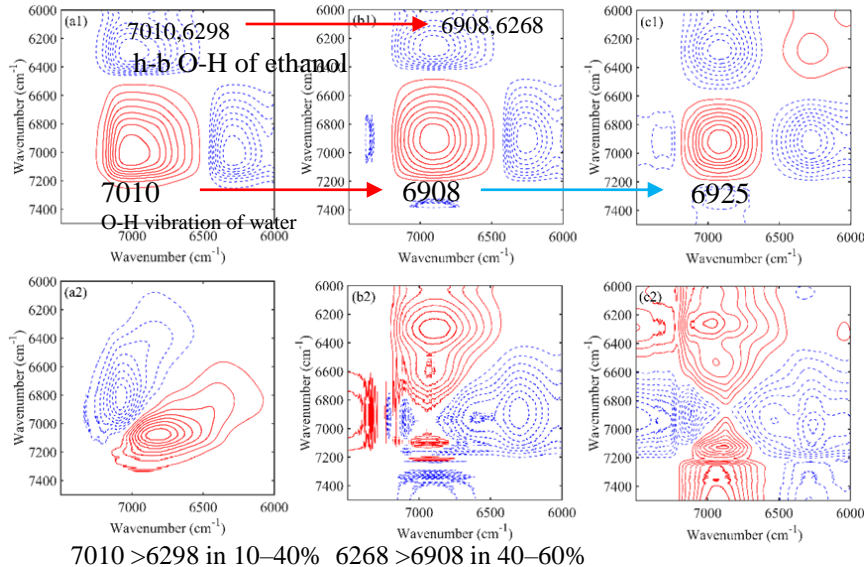
The result indicates that the free O-H in water is least in 40% ethanol-water mixtures and O-H in water achieves the maximum participation in hydrogen bonding interaction. The hydrogen bonding strength in the mixtures reaches the maximum at 40% ethanol concentration and is almost constant in 40-60% mixtures.

Figure 7. The intensity variation of the excess peaks at 7080 cm⁻¹ (a) and 6420 cm⁻¹ (b) with ethanol concentration.

应用简介-近红外结合水光谱用于水醇体系的研究

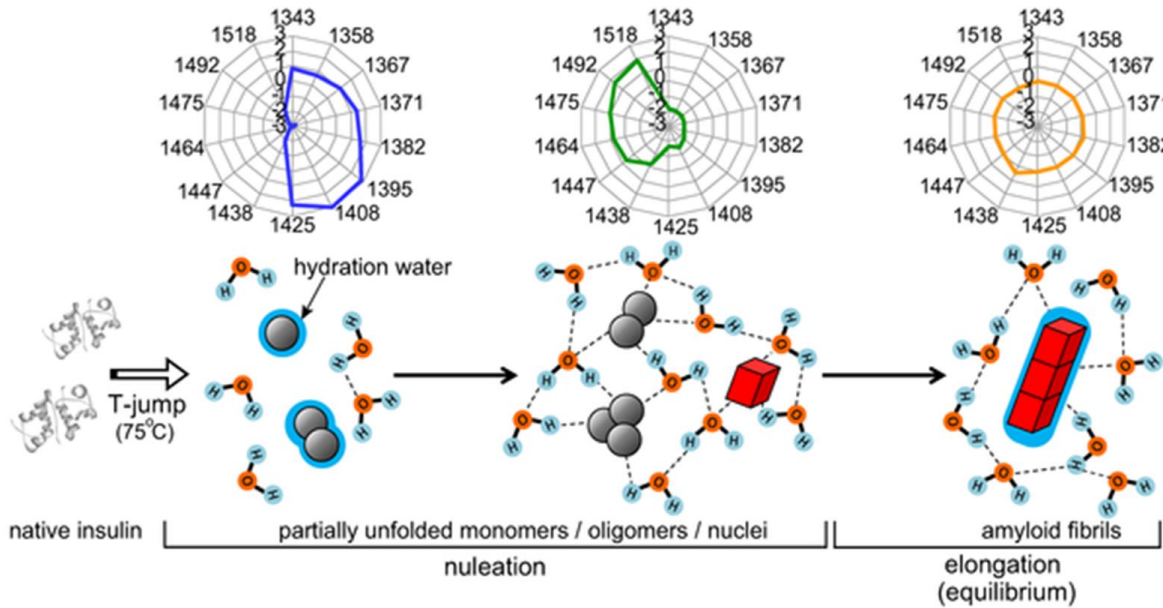


Analysis of ethanol-water mixtures in the range of 10-100% ethanol concentration



Various studies have reported anomalous properties of some of the parameters in ethanol-water mixtures around 40% concentration, such as excess mixing enthalpies, negative adiabatic compressibility coefficient and fluorescence quenching. Presumably, the maximum involvement of O-H groups of water in hydrogen bonding and the self-association in ethanol molecules may be the reason of these anomalous properties.

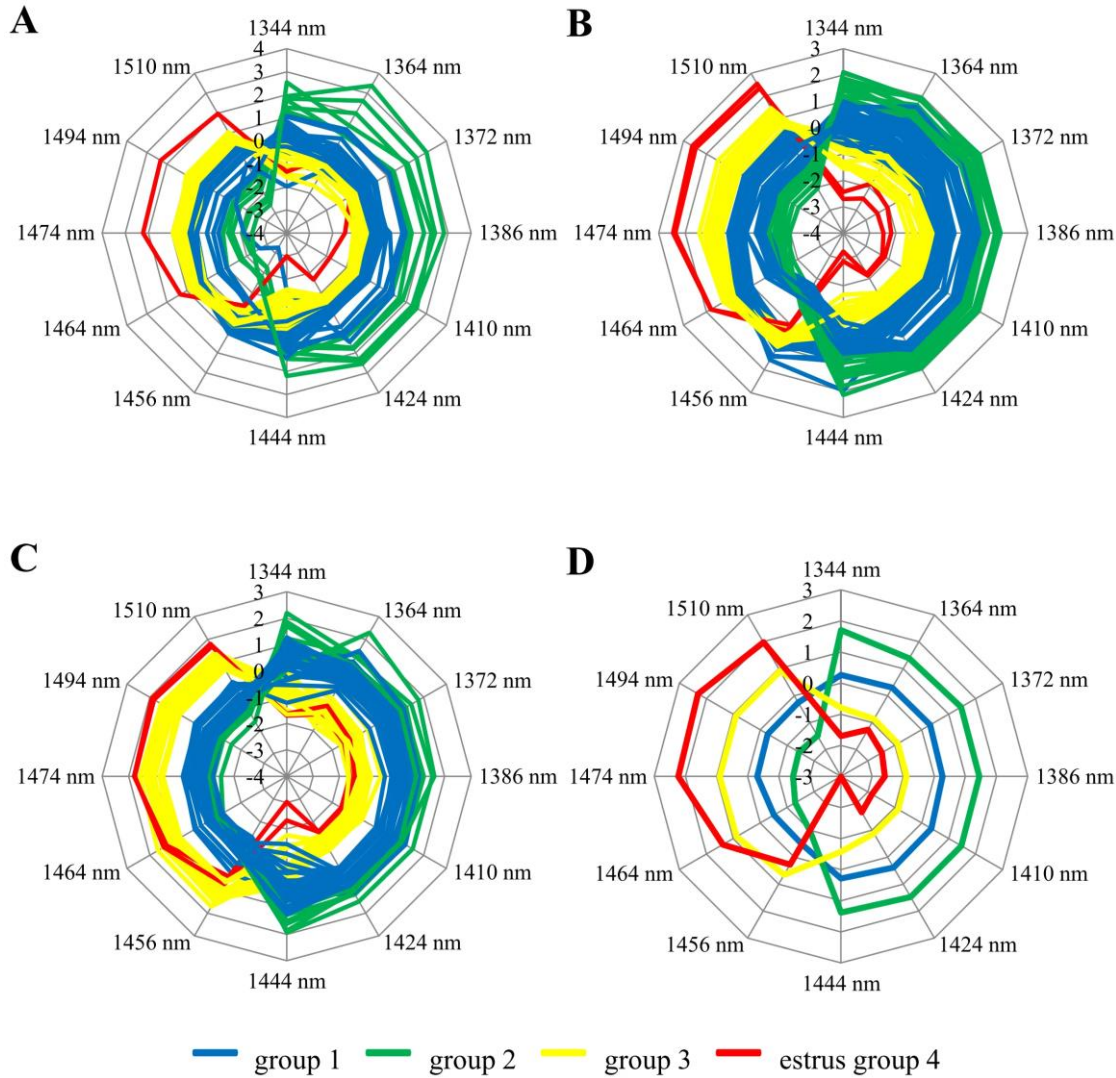
Fig.8 Synchronous (1) and asynchronous (2) 2D correlation spectra of 10-40% (a), 40-60% (b), and 60-100% (c) ethanol-water mixtures. The solid red lines denote the positive sign and the dashed blue lines denote the negative sign.

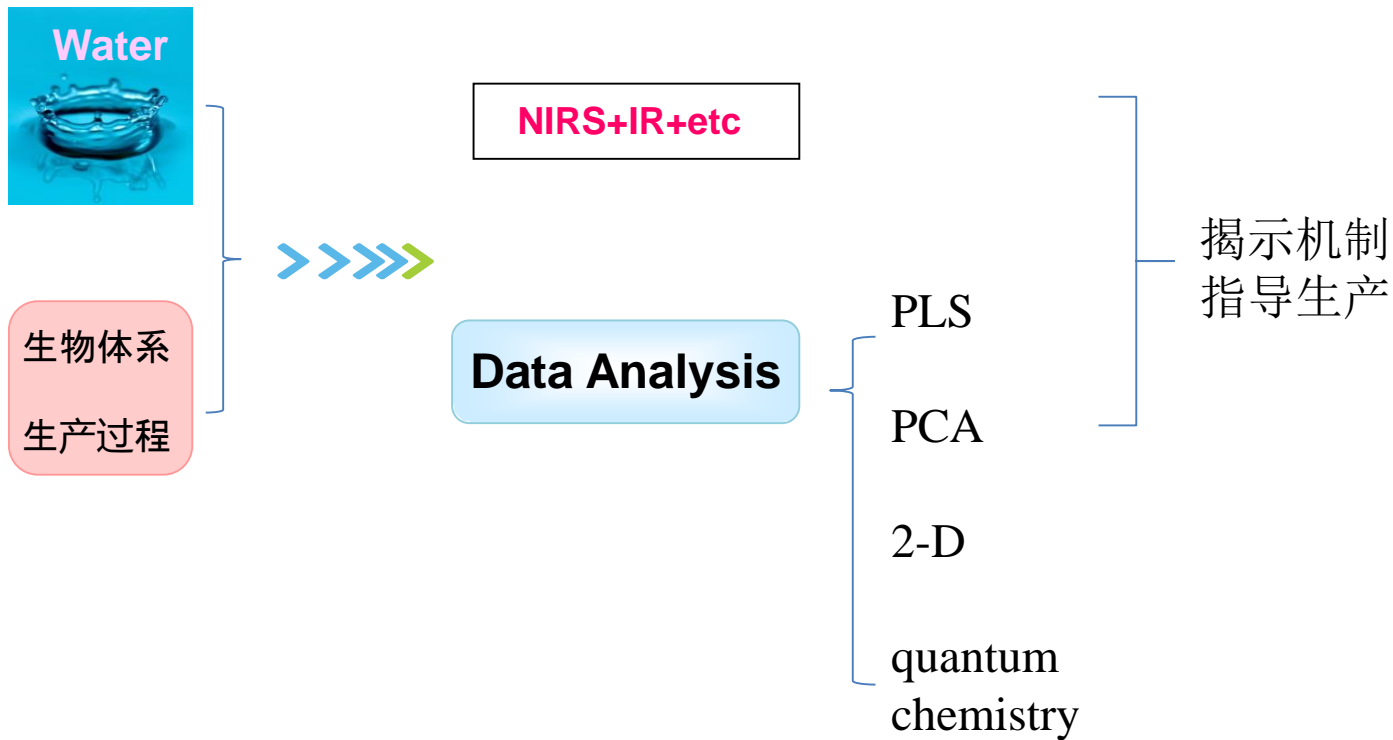


In the nucleation phase, free water molecules and hydrating water onto protein molecules are dominated initially, but afterwards hydrogen-bonded water networks are developed, which is considered essential for nucleation by interlinking protein molecules softly. In the elongation phase, the hydrogen bonds were decayed gradually towards the

Figure: Schematic illustration representing multi-step transformation of water structures during the fibril formation.

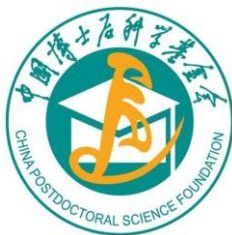
应用简介-其它







山东大学药学院
SCHOOL OF PHARMACEUTICAL SCIENCES
SHANDONG UNIVERSITY



山东大学
SHANDONG UNIVERSITY